

Gas Sensing Characteristics of a WO₃ Thin Film Prepared by a Sol-Gel Method †

Mitsuaki Yano *, Tomoya Iwata, Satoshi Murakami, Ryouma Kamei, Taichi Inoue and Kazuto Koike

Nanomaterials and Microdevices Research Center, Osaka Institute of Technology, Asahi-ku Ohmiya, Osaka 535-8585, Japan; m1m17303@st.oit.ac.jp (T.I.); m1m17337@st.oit.ac.jp (S.M.); m1m17310@st.oit.ac.jp (R.K.); m1m18304@st.oit.ac.jp (T.I.); kazuto.koike@oit.ac.jp (K.K.)

* Correspondence: mitsuaki.yano@oit.ac.jp; Tel.: +81-6-6954-4313

† Presented at the Eurosensors 2018 Conference, Graz, Austria, 9–12 September 2018.

Published: 4 December 2018

Abstract: Preparation and characterization of a WO₃-based thin film gas sensor are reported. The WO₃ film was prepared on a polished alumina substrate by a sol-gel method using an aqueous mixture solution of ammonium metatungstate hydrate and poly-vinyl alcohol, and fabricated into the gas sensor by forming interdigital electrodes on the surface. The characterization was conducted by measuring the electrical resistance change in NO, H₂, and NH₃ ambient as a function of gas concentration. It is revealed that the sensor has a specific sensitivity to NO, NO is detected as oxidizing gas although it is expected to be reducing gas, and the resistance changes with gas concentration in accordance with the Langmuir isotherm plot.

Keywords: gas sensor; sensing mechanism; NO gas; WO₃; sol-gel method

1. Introduction

It is important to monitor the pollutant NO_x concentration in exhaust and livestock production gases, which has promoted vigorous study on WO₃ for the application to NO_x gas sensors. For this purpose, WO₃ films were prepared by such many techniques as sputtering [1], thermal evaporation [2], pulsed laser deposition [3] and sol-gel [4,5] methods. Among them, sol-gel is the most promising candidate method for the capability of low cost fabrication in large area since it is a typical technique of non-vacuum processing. In this study, we fabricated a gas sensor from a WO₃ thin film prepared by a sol-gel method using an aqueous mixture solution of cost-effective popular reagents; ammonium metatungstate hydrate (AMT) and poly-vinyl alcohol (PVA).

From the viewpoint of the systematic understanding of sensing mechanism, on the other side, not enough effort is devoted for WO₃-based gas sensors to discuss the detection characteristics using common physicochemical parameters while many works have been concentrated to increase the sensitivity. To contribute to the systematic understanding, we analyzed the detection characteristics of our WO₃-based gas sensor by measuring the response to NO, H₂, and NH₃. NO was chosen as the representative of NO_x because it is used as the indicator of photochemical smog and is the precursor of NO₂. Since NO (reducing gas) is rapidly converted to NO₂ (oxidizing gas) in air, we compared the response to NO with that to conventional reducing gases of H₂ and NH₃ to clarify the detection mechanism. We also analyzed the sensing behavior by modeling the resistance change using the Schottky barrier at grain boundaries and the Langmuir isotherm adsorption of ambient gas [6].

2. Experimental Procedure

To estimate the optimal calcination temperature of the sol-gel processing, thermogravimetry-differential thermal analysis (TG-DTA) was conducted for 50 w% aqueous solution of AMT (Japan New Metals) and 10 wt % aqueous solution of PVA (Fuji Film Wako) using a Seiko Instruments-made TG-DTA 6300 system. As shown in Figure 1a,b), water evaporates at around 100 °C for both cases, AMT decomposes at around 300 °C and crystallizes into WO₃ at around 500 °C, and PVA burns out at around 550 °C. From these results, we used 600 °C for the calcination temperature in the following experiment.

The WO₃ film for the gas sensor was prepared on a polished alumina substrate (Maruwa) with 40 nm root-mean-square (RMS) surface roughness. First, an aqueous mixture solution of PVA:AMT:H₂O = 1:20:300 (in wt %) was coated on the alumina surface using a spin-coating method at 2000 rpm for 30 s. Then the film was dried at 200 °C for 10 min in air, and the calcination at 600 °C was conducted for 2 h in air, resulting in an approximately 50 nm thick WO₃ thin film without cracks.

The following basic properties were obtained for the equivalent WO₃ film prepared on a glass substrate (Corning EAGLE XG) using the same fabrication procedure. The X-ray diffraction (XRD) measurement in 2^θ/ω configuration using a Rigaku-made SmartLab system with Cu K 1 radiation indicated that the WO₃ film was crystallized in an *a*-axis oriented orthorhombic polycrystalline phase. The X-ray reflection measurement using the same XRD system combined with a simulation software (Rigaku GlobalFit) indicated that the film was 47 nm in thickness, 0.79 nm in RMS roughness, and 7.1 g/cm³ in density, in good agreement with the data measured by an atomic force microscope (Shimadzu SPM-9700) of 45 nm in thickness and 0.56 nm in RMS roughness, and with the well-known WO₃ density of 7.16 g/cm³, showing that the film was solid and neither porous nor granular. The bandgap energy determined by the Tauc plot of the optical transmittance at 300 K assuming indirect transition was 2.8 eV in consistent with the value for bulk WO₃. The Hall effect measurement by van der Pauw method indicated that the conduction was *n*-type with a carrier concentration of about 2 × 10¹⁶ cm⁻³ and a mobility of about 30 cm²/Vs.

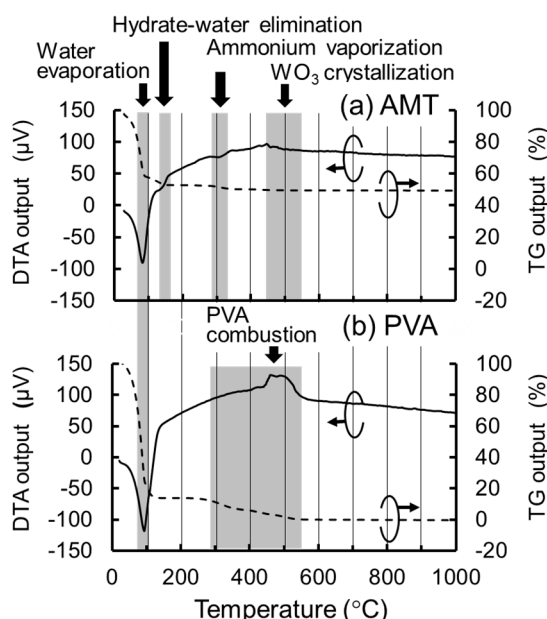


Figure 1. TG-DTA curves in air of the components of precursor aqueous solutions; AMT and PVA. It is indicated by (a) that AMT decomposes at around 300 °C and crystallizes at around 500 °C, and by (b) that PVA burns out at around 550 °C.

The fabrication process of the gas sensor with interdigital electrodes (IDEs) is given in Figure 2. The IDEs were formed by evaporating a Au (150 nm)/In (20 nm) film on the WO₃ surface where the In thin layer was inserted to improve contact resistance, and by patterning their nine-pairs of finger electrodes using a lift-off technique combined with standard photolithography. The dimensions of the finger electrodes were 1.8 mm in width and 50 μm in line and space.

The gas sensing characteristics were measured in a flow-type airtight test fixture where the gas sensor was mounted side-by-side with a dummy sample on an alumina-made heating block. We bonded a thermo-couple on the dummy surface and connected it to an outside PID controlled power supply for the heating block. Electrical leads were bonded to the IDEs on the sensor surface to connect with an outside digital multimeter (Keysight 34465A) by using a glass frit Ag glazing paste (Daiken Chemical). The concentration of NO, NH₃, and H₂ gases (Air Water) was adjusted in the range of 1.0–1000 ppm by using Horiba-made mass-flow controllers and clean air gas (99.99%, 21 vol% O₂ in N₂) for dilution with a total flow rate of about 1 L/min.

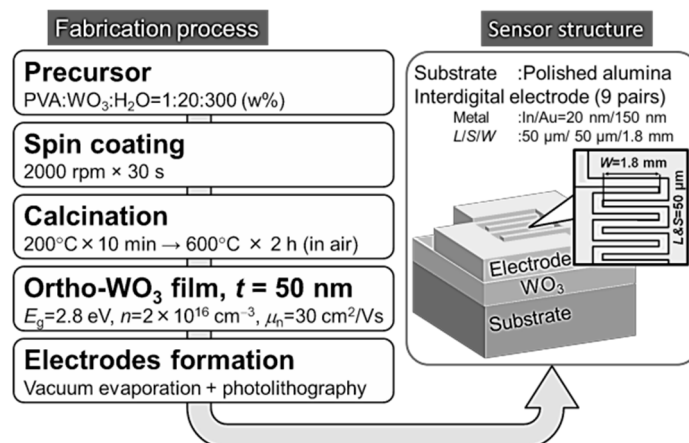


Figure 2. Fabrication process of the WO₃-based gas sensor. A 50 nm thick *n*-type WO₃ film was formed on a alumina substrate using a sol-gel method, and it was fabricated into a gas sensor with IDEs. The dimensions of the finger electrodes are given in the figure.

3. Gas Sensing Characteristics

The model band-diagram at the grain boundaries in WO₃ film is depicted in Figure 3, where the symbols of ϕ_0 , ϕ_{Ox} and ϕ_{Re} represent the Schottky barrier heights at the stationary states in clean air, oxidizing gas, and reducing gas, respectively. In clean air, a considerable part of the grain surface is covered with oxygen atoms which are negatively charged by capturing the conduction electrons in WO₃. The Schottky barrier with a height of ϕ_0 is formed to compensate the negative surface charges with the positively charged donors in the depletion layer. When reducing gas reacts with the negatively charged oxygen atoms, the depletion width will be reduced by lowering the barrier height, while the reaction of the grain surface with oxidizing gas enhances the depletion width by increasing the barrier height.

The relationship between the barrier height ϕ and the concentration of the negative charge C at the grain surface is given by solving the following equations,

$$\phi = \frac{q}{\epsilon_s} \int_0^{x_d} (-C + N_D x) dx, \text{ and } C = N_D x_d \quad (1)$$

where q is the electron charge, ϵ_s is the dielectric constant of WO₃, N_D is the donor concentration in WO₃, x is the distance from the surface toward the inside, and x_d is the edge position of the depletion layer. We obtain the relationship,

$$\phi = -qC^2/2\epsilon_s N_D. \quad (2)$$

When the concentration of effective charge is changed from the initial value C_0 in clean air to $C = C_0 + \Delta C$ after gas adsorption, the increase of the barrier height $\Delta\phi$ assuming $C_0 \gg \Delta C$ is expressed as

$$\Delta\phi = qC_0\Delta C/\epsilon_s N_D \quad (3)$$

where $\Delta C > 0$ for oxidizing gas and $\Delta C < 0$ for reducing gas. Accordingly, the electron concentration n that can get over the Schottky barrier after gas adsorption is expressed as

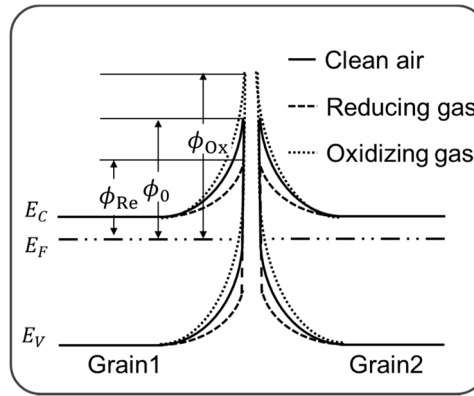


Figure 3. Schematic band-diagram at around the grain boundaries in *n*-type WO₃ films. The Schottky barrier for conduction electrons becomes high under the adsorption of oxidizing gas, and low under that of reducing gas.

$$n = n_0 \exp(-q\Delta\phi/kT) = n_0 \exp(-q^2 C_0 \Delta C / kT \epsilon_s N_D) \quad (4)$$

where n_0 is the electron concentration that can get over the Schottky barrier in clean air, k is the Boltzmann constant, T is the absolute temperature. Assuming that the electron mobility does not depend on n , the electrical resistance R_G after gas absorption becomes

$$R_G = R_0 \exp(q^2 C_0 \Delta C / kT \epsilon_s N_D) \quad (5)$$

where R_0 is the resistance in clean air. Then, we obtain the relationship

$$\Delta \ln R = \ln(R_G/R_0) = q^2 C_0 \Delta C / kT \epsilon_s N_D \quad (6)$$

Therefore, we can expect that $\Delta \text{Log}R$ is directly proportional to ΔC , and that the resistance change in logarithmic scale increases and decreases with the increase of oxidizing and reducing gas adsorption, respectively.

If the change of the effective charge ΔC is yielded only by the monolayer adsorption and the adsorption sites are distributed randomly on the WO₃ surface, the coverage θ of the adsorbed gas molecules will be expressed as follows using the Langmuir isotherm equation,

$$\theta = \frac{\Delta C}{\Delta C_{\max}} = \frac{\Delta \text{Log}R}{\Delta \text{Log}R_{\max}} = \frac{K C_G}{1 + K C_G} \quad (7)$$

where ΔC_{\max} is the maximum adsorption capability, $\Delta \text{Log}R_{\max}$ is the resistance change at $\theta = 1$, C_G is the equilibrium concentration of oxidizing or reducing gas in air, $1/K$ is the dissociation constant. As the result, we can expect a sigmoidal curve for the dependence of $\Delta \text{Log}R$ on C_G .

The experimental results at 300 °C are shown by the $\Delta \text{Log}R$ plots as a function of C_G in Figure 4. Each value of $\Delta \text{Log}R$ was obtained by measuring the saturated resistance change after ten minutes or more from the introduction of a certain gas concentration; where the response time required for 63% change in $\Delta \text{Log}R$ was less than several minutes. Lines in Figure 4, on the other hand, are the fitting curves calculated from Equation (7) of which values $1/K$ and $\Delta \text{Log}R_{\max}$ are estimated as follows; $1/K = 4.9 \times 10^{-5}$ and $\Delta \text{Log}R_{\max} = 2.8$ for NO, $1/K = 2.6 \times 10^{-4}$ and $\Delta \text{Log}R_{\max} = -0.23$ for H₂, and $1/K = 2.9 \times 10^{-5}$ and $\Delta \text{Log}R_{\max} = -0.17$ for NH₃ by fitting the experimental data to the Hanes-Woolf plot. One can see in Figure 4 a good agreement of the calculation with the experiment, indicating that the resistance change can be interpreted by the simple model mentioned above.

It is denoted by the positive sign of $\Delta \text{Log}R_{\max}$ that NO is detected as a kind of oxidizing gas similar to the report by others [7] presumably due to the immediate oxidization in air/on WO₃ surface, which is very different from the cases of H₂ and NH₃. It is also shown by the much larger $\Delta \text{Log}R_{\max}$ value of NO that WO₃ has a specific sensitivity to NO_x. In order to shift the sigmoidal curve toward the lower gas concentration, reduction of the dissociation constant, $1/K$, by using additives with catalytic function will be effective. As well, the use of nanostructured/porous WO₃ films can be

helpful for the improvement of the sensitivity and response time by reducing the contribution from the insensitive deeper layers in WO_3 , while the presented data were taken for a solid and flat film without additives to study the basic properties of WO_3 -based gas sensors.

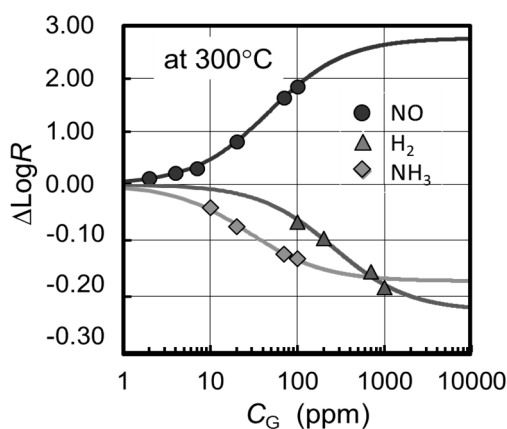


Figure 4. Experimental results at 300 °C (plots) and their fitting curves (lines) to the Langmuir isotherm plot as a function of the concentration of NO , H_2 , and NH_3 . Note that the scale of the negative side in vertical axis is one decade smaller than that of the positive side.

Funding: A part of this work was funded by JSPS KAKENHI Grant Numbers 16K04936 and 17K06472.

Conflicts of Interest: The authors declare no conflict of interest.

References

- Kim, T.S.; Kim, Y.B.; Yoo, K.S.; Sung, G.S.; Jung, H.J. Sensing characteristics of dc reactive sputtered WO_3 thin films as an NO_x gas sensor. *Sens. Actuators* **2000**, *B62*, 103–108.
- Lee, D.-S.; Nam, K.-H.; Lee, D.-D. Effect of substrate on NO_2 -sensing properties of WO_x thin film gas sensors. *Thin Solid Films* **2000**, *375*, 142–146.
- Kawasaki, H.; Namba, J.; Iwatsuji, K.; Suda, Y.; Wada, K.; Ebihara, K.; Ohshima, T. NO_x gas sensing properties of tungsten oxide films synthesized by pulsed laser deposition method. *Appl. Surf. Sci.* **2002**, *197*, 547–551.
- Teoh, L.G.; Hon, Y.M.; Shieh, J.; Lai, W.H.; Hon, M.H. Sensitivity properties of a novel NO_2 gas sensor based on mesoporous WO_3 thin film. *Sens. Actuators* **2003**, *B96*, 219–225.
- Breedon, M.; Spizzirri, P.; Taylor, M.; Plessis, J.D.; McCulloch, D.; Zhu, J.; Yu, L.; Hu, Z.; Rix, C.; Wlodarski, W.; et al. Synthesis of nanostructured tungsten oxide thin films: A simple, controllable, inexpensive, aqueous sol-gel method. *Cryst. Growth Des.* **2010**, *10*, 430–439.
- Yano, M.; Hirahara, Y.; Terada, J.; Sasa, S.; Omatu, S. Characteristics of p-type semiconducting MgCr_2O_4 - TiO_2 ceramics for gas sensing devices. *IEEJ Trans. Sens. Michromach.* **2015**, *135*, 317–322. (In Japanese).
- Akamatsu, T.; Itoh, T.; Izu, N.; Shin, W. NO and NO_2 sensing properties of WO_3 and Co_3O_4 based gas sensors. *Sensors* **2013**, *13*, 12467–12481.



© 2018 by the authors. Licensee MDPI, Basel, Switzerland. This article is an open access article distributed under the terms and conditions of the Creative Commons Attribution (CC BY) license (<http://creativecommons.org/licenses/by/4.0/>).